International Institute for Applied Systems Analysis
IIASA www.iiasa.ac.at

Estimation of GCM Temperature Trends for Different Emission Scenarios with the help of the Integrated Model to Assess the Greenhouse Effect (IMAGE)

Fleischmann, K., Nitschke, U., Jonas, M., Olendrzynski, K. and Shaw, R.W.

IIASA Working Paper

WP-92-011

January 1992

Working Paper

Estimation of GCM Temperature Trends for Different Emission Scenarios with the help of the Integrated Model to Assess the Greenhouse Effect (IMAGE)

Katharina Fleischmann
Uta Nitschke
Matthias Jonas
Krzysztof Olendrzyński
Roderick W. Shaw

WP-92-11
January 1992

IIASA International Institute for Applied Systems Analysis □ A-2361 Laxenburg □ Austria
Telephone: +43 2236 715210 □ Telex: 079 137 iiasa a □ Telefax: +43 2236 71313

Estimation of GCM Temperature Trends for Different Emission Scenarios with the help of the Integrated Model to Assess the Greenhouse Effect (IMAGE)

Katharina Fleischmann
Uta Nitschke
Matthias Jonas
Krzysztof Olendrzyński
Roderick W. Shaw

WP-92-11
January 1992

International Institute for Applied Systems Analysis □ A-2361 Laxenburg □ Austria
Telephone: +43 2236 715210 □ Telex: 079 137 iiasa a □ Telefax: +43 2236 71313

FOREWORD

IIASA, in collaboration with the National Institute for Public Health and Environmental Protection (RIVM; Bilthoven, The Netherlands), is adapting RIVM's Integrated Model to Assess the Greenhouse Effect (IMAGE) to provide regional values of temperature and, eventually, precipitation change resulting from a variety of greenhouse gas scenarios. These regional values will be used as input to impact models such as those for vegetation and forest growth that are being developed at IIASA. One approach, described in a recent Collaborative Paper by Jonas, den Elzen and Olendrzyński entitled "A Time-dependent Zonally Averaged Energy Balance Model to be Incorporated into IMAGE" described the development of an Energy Balance Model to achieve these ends with respect to temperature. A parallel approach, to be described in this Working Paper, is to combine the time-dependent surface temperature outputs of IMAGE for a large number of greenhouse gas scenarios with the spatial resolution of General Circulation Models. This paper reports on some of the basic concepts that have been developed for the second approach which will be applied in 1992 and 1993.

ABSTRACT

How useful are General Circulation Models (GCMs) for policy makers? Of course, they are considered to be the most powerful models that are presently available for predicting future climates and for carrying out research. Their disadvantage is that they are very time-consuming and very expensive to run for any greenhouse gas emission or concentration scenario. For that reason, GCMs have been run only for a small number of scenarios. However, policy makers are interested in being able to analyze a large number of scenarios. The Integrated Model to Assess the Greenhouse Effect (IMAGE) developed by the National Institute for Public Health and Environmental Protection (RIVM) in the Netherlands is a scientifically based, policy oriented model that can calculate the effect of different greenhouse gas emissions on global surface air temperature and sea level rise. The major advantage of IMAGE is its quick turnaround time. Its disadvantage is that it gives only global values of surface temperature and sea level rise, which have insufficient spatial resolution to estimate ecological impacts on a regional basis. We propose a methodology for combining the fast turnaround time and time-dependent surface temperature results of IMAGE with the spatial resolution of GCMs to provide a linkage between IMAGE and models of ecological change that could provide policy-makers with valuable information about the consequences of different levels of reduction of greenhouse gas emissions.

TABLE OF CONTENTS

1. INTRODUCTION AND BACKGROUND

1.1. Purpose of the work

The purpose of this paper is to outline a methodology for combining the surface temperature outputs of three-dimensional General Circulation Models (GCMs) with those of a zero-dimensional but time-dependent policy-oriented model, the Integrated Model to Assess the Greenhouse Effect (IMAGE). The temperature outputs of GCMs give detailed projections of climatic change far into the future. They can do this for only a few scenarios of atmospheric greenhouse gas concentrations because of the huge computational time required even on supercomputers. For example, the GCM of the Max-Planck-Institut for one-year integration requires 8 to 12 hours on one processor of the CRAY-2 system (Cubasch et al., 1991). IMAGE, on the other hand, can rapidly assess the effects of numerous emission or concentration scenarios due to its quick turnaround time, but it gives only global temperature change. Our ultimate aim is to produce a tool which takes advantage of both models and which can be linked to models of ecological effects such as vegetation and forestry models. Quick turnaround climate models resolving surface temperature in space and time are thought to be most useful to decisionmakers and research groups dealing with subsequent impact studies (cf. Figure 1).

1.2. General Circulation Models (GCMs)

General Circulation Models are used to simulate changes in the global climate by attempting to simulate the hour-by-hour evolution of the atmosphere in all three spatial dimensions. The simulations are based on the conservation laws for atmospheric mass, momentum, total energy and water vapor. Important feedback mechanisms are included explicitly. GCMs also typically include representations of surface hydrology, sea ice, cloudiness, convection, atmospheric radiation and other processes. If processes which are smaller than the spatial grid are considered, then they are parameterized statistically or empirically.

The most sophisticated of the GCMs are the coupled atmospheric oceanic GCMs, since they model the flux processes not only in the atmosphere but also in the ocean. The incorporation of the three-dimensional ocean circulation results in a temperature increase which in general is smaller than if ocean circulation were not included in the model. Possible changes in the ocean circulation, in turn, lead to changes in the atmospheric circulation. Therefore it is necessary to simulate both the atmospheric and the oceanic circulation as a coupled system giving full treatment to ocean momentum, salinity and thermal energy. Today there are about five coupled ocean-atmospheric GCMs, which resolve the deep ocean in detail. These five models are (WCRP-55,1991):

- GFDL (Geophysical Fluid Dynamics Laboratory) coupled ocean-atmosphere model (Stouffer, 1989)

- NCAR (National Center for Atmospheric Research) global coarse-grid coupled ocean-atmosphere model (Meehl and Washington, 1989)

- MPI model of the Max-Planck-Institut für Meteorologie, Hamburg (Cubasch et al., 1990)

- UHH model of the University of Hamburg (Oberhuber et al., 1990)

- UKMO (United Kingdom Meteorological Office) global coupled ocean-atmosphere climate model (Mitchell et al.,1990)

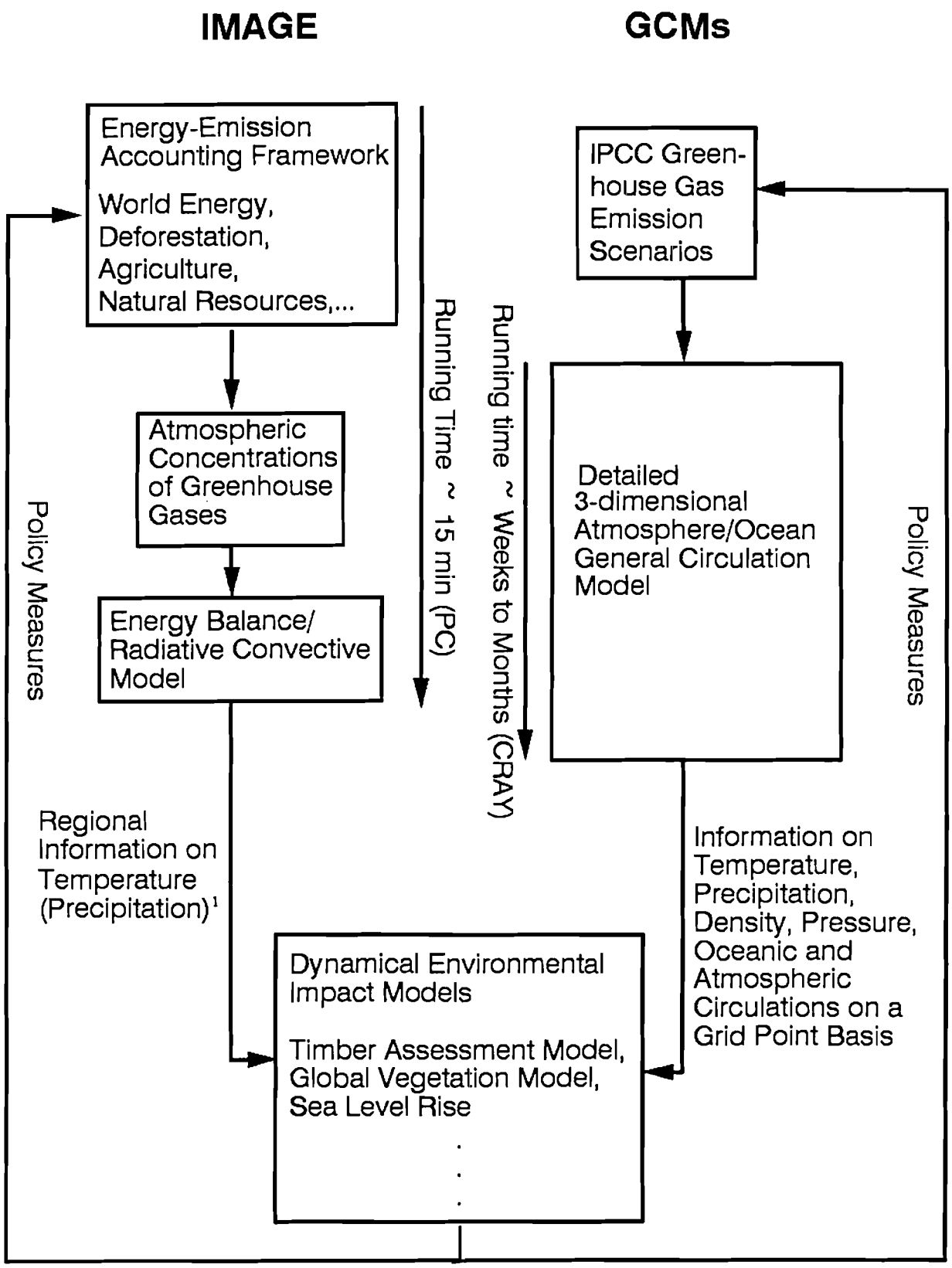

Figure 1: Schematic illustration: Comparison of GCMs and IMAGE.

[1] This does not apply to the present version of IMAGE. In collaboration with RIVM the climate module of IMAGE is being regionalized by IIASA's Climate Change Strategies Project

The development of the present comprehensive GCMs which take into account all components of the climate system (atmosphere, ocean, land-surface and cryosphere) were preceeded by more simple models which took into account the effect of the ocean in a very simplified way, e.g. by letting the ocean be represented by a slab which could store heat and act as a moisture source. More sophisticated slab ocean models attempt to parameterize the 2-dimensional dynamical behavior of the ocean (horizontal and vertical currents) through the prescription of heat convergence or divergence (Harrison, 1990).

The terminology of GCM model runs according to the Intergovernmental Panel on Climate Change (IPCC) is shown in Figure 2. It distinguishes between instantaneous doubling of the CO_2 equivalent[2] concentration (CO_2 equivalent) and a gradually varying concentration in the atmosphere. The term *equilibrium run* usually stands for so called "switch-on" experiments (instantaneous doubling of CO_2 equivalent concentration) that ignore both the deep ocean and changes in the ocean circulation, and the resulting time delays; these runs represent a system in equilibrium. The *transient runs* are switch-on experiments that take the ocean into account so that the evolution with time of the whole climate system could be examined. However, for very sophisticated coupled GCMs, the equilibrium state of the climate systems may not be reached, because of limited computing time. *Time-dependent runs* are based on gradually varying CO_2 equivalent concentrations; the concentrations are actually changing in this way within the real climate system (IPCC,1990).

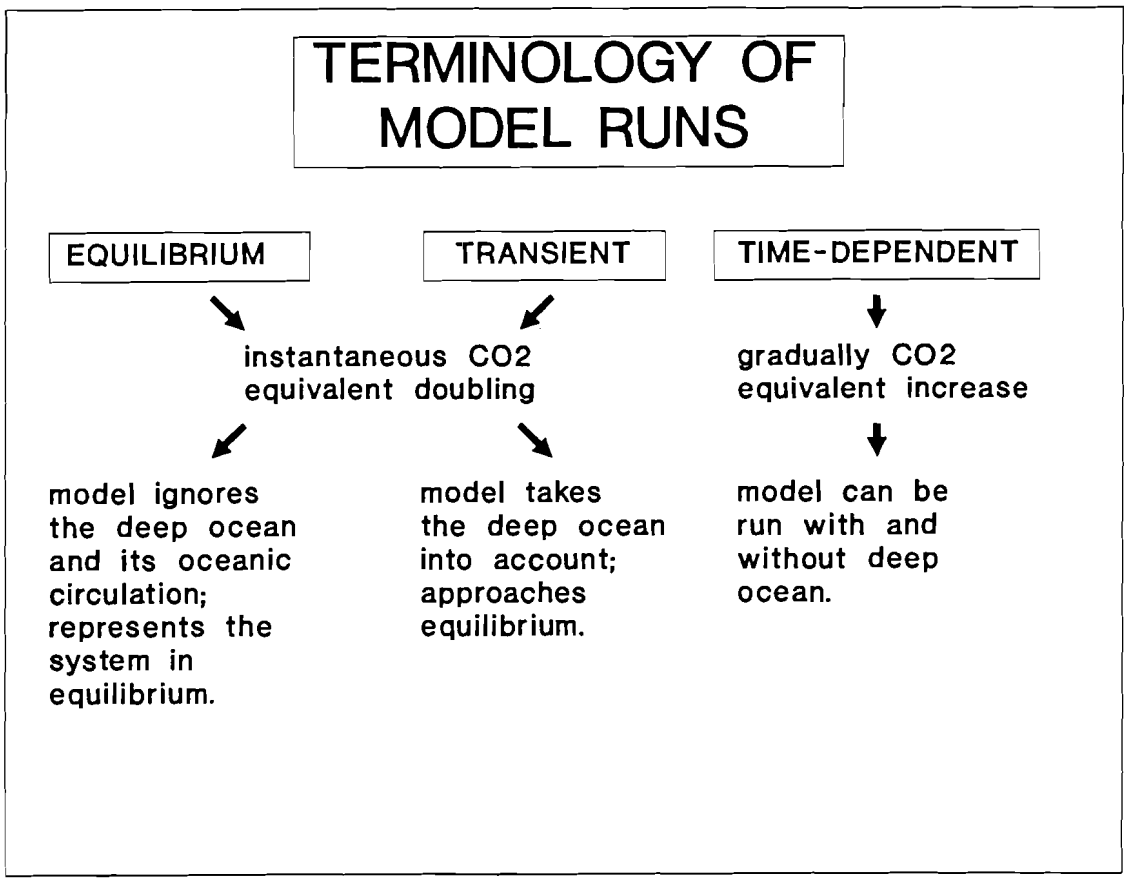

Figure 2: Terminology of GCM runs.

---

[2] The CO_2 equivalent concentration is often used to sum up the contribution of all greenhouse gases which affect the radiation balance of the atmosphere: CO_2, CH_4, O_3, N_2O, CFC-11, CFC-12 and others.

The various research groups which are engaged in simulating the effect of an increase of the equivalent atmospheric concentration of greenhouse gases use somewhat different values for the initial equivalent atmopheric concentration of CO_2 (the year for its doubling will therefore also be different): GFDL uses 300 ppmv as an initial value, NCAR uses 330 ppmv, MPI/UHH 360 ppmv, and UKMO 323 ppmv.

1.3. Integrated Model to Assess the Greenhouse Effect (IMAGE)

Since it is too expensive and time consuming to run GCMs for a large number of concentration scenarios, simpler models have been developed. One such example is the Integrated Model to Assess the Greenhouse Effect (IMAGE) developed by the National Institute for Public Health and Environmental Protection (RIVM) in the Netherlands (Rotmans, 1990). IMAGE is based on a zero-dimensional but time-dependent Energy Balance Model (EBM) and can be used for the calculation of historical and future concentrations of greenhouse gases, and of the effects on global temperature and sea level rise. It consists of the different modules depicted in Figure 3. A more detailed structure of IMAGE is given in Figure 4.

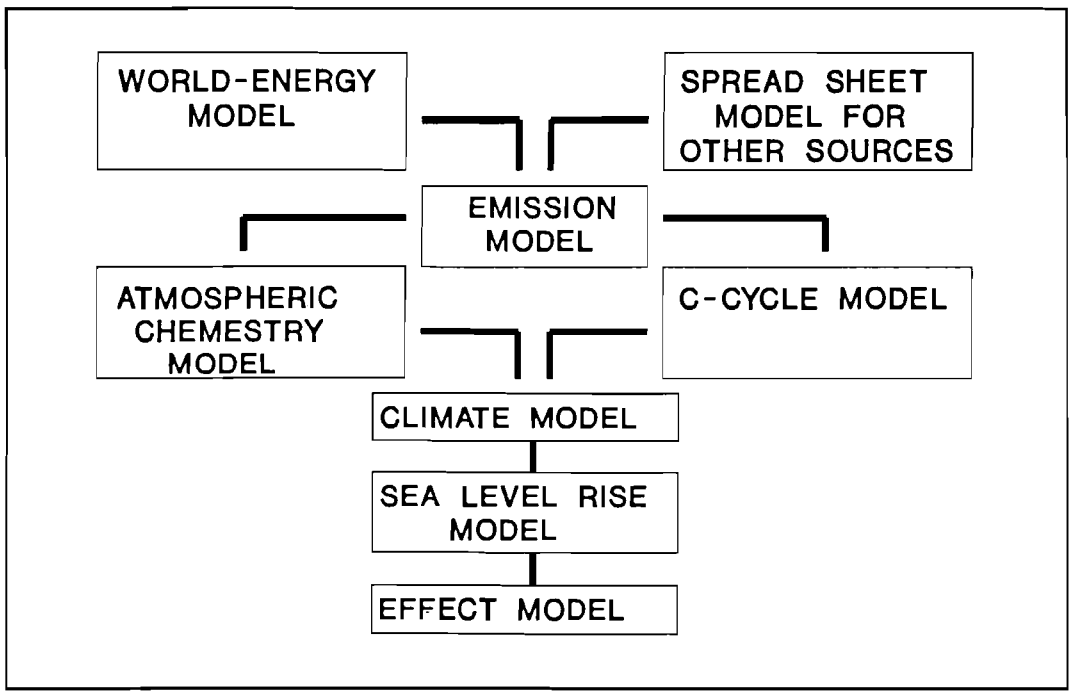

Figure 3: IMAGE modules (Rotmans,1990). See Figure 4 for details.

The advantage of IMAGE is that it calculates the temperature change more quickly and cheaply than GCMs; it is therefore a useful tool for policymakers to assess what measures should be taken to limit climate change. IMAGE provides only one global value (or possibly one for each hemisphere) for the temperature change. However, to assess ecological impacts of climate change, temperature values with a finer geographical resolution are needed.

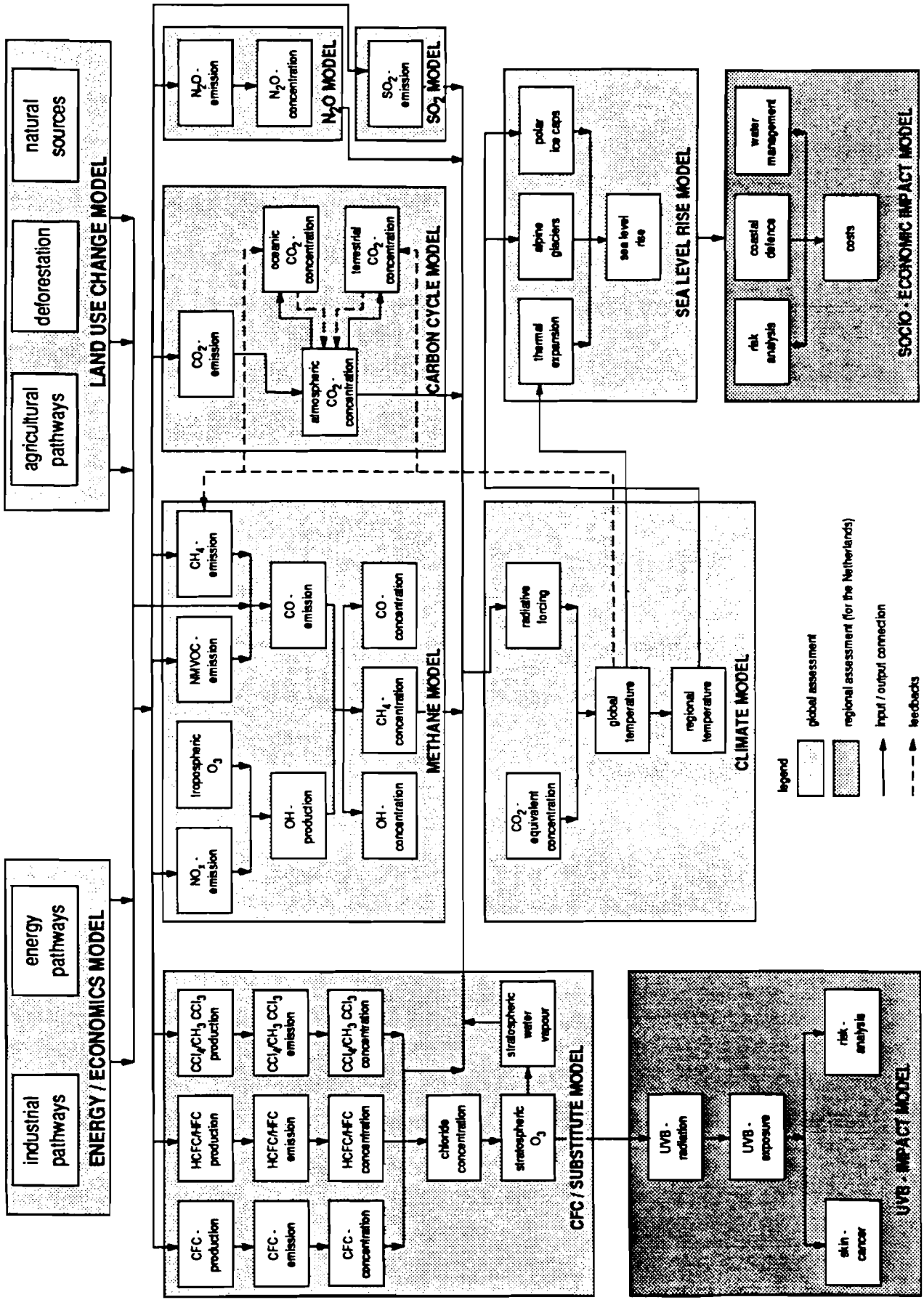

Figure 4: Detailed structure of IMAGE (Rotmans et al., 1991).

1.4. Description of concentration scenarios

Concentration scenarios are used as input to models of climate change. They describe the atmospheric concentrations of greenhouse gases from the present time to the year 2100. For the future the most commonly used ones are Scenarios A,B,C and D, as calculated by IMAGE and used by the Intergovernmental Panel on Climate Change (IPCC). These four scenarios are based on different assumptions about the development of energy supply, efficiency, deforestation, emissions from agriculture, and the implementation of the Montreal Protocol.

Figure 5 shows how the atmospheric CO_2 equivalent concentrations change with time in the four scenarios as calculated by IMAGE.

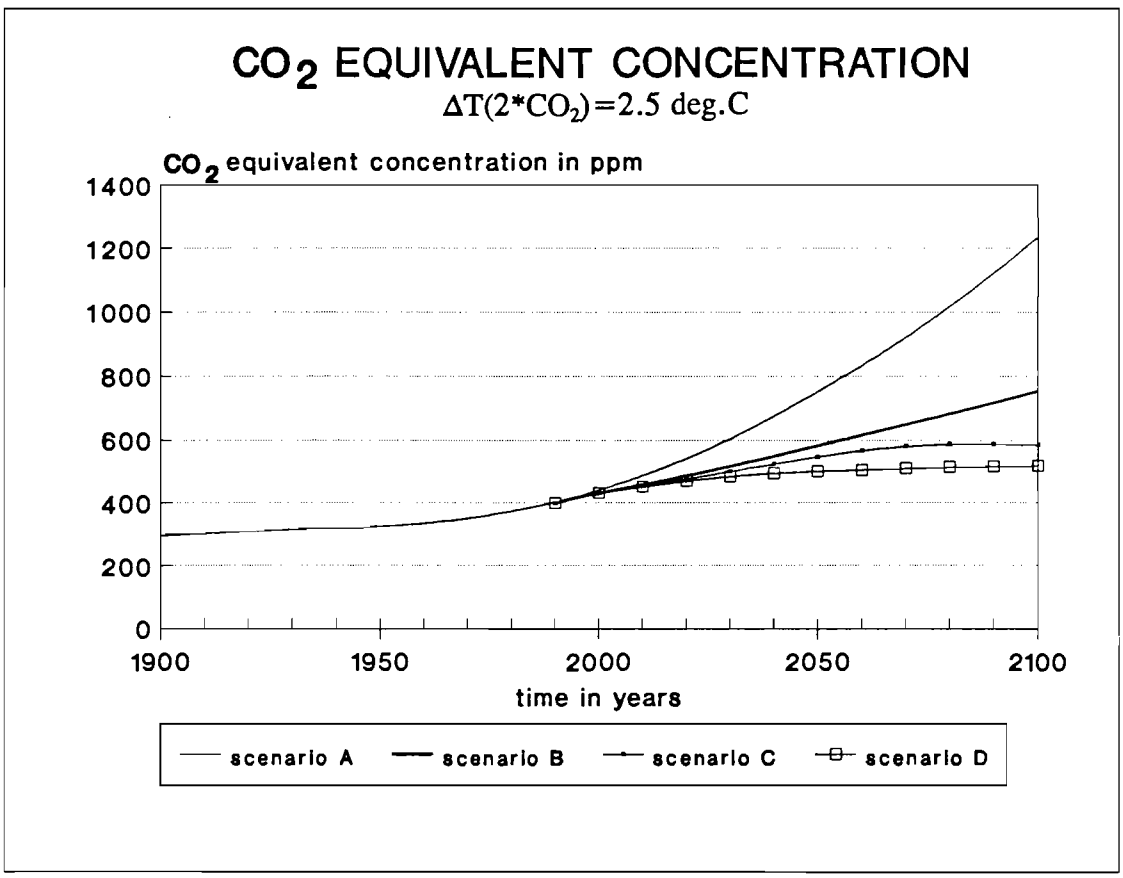

Figure 5: CO_2 equivalent concentration Scenarios A, B, C, D for the climate sensitivity[3] $\Delta T(2*CO_2)=2.5°C$.

[3] The climate sensitivity $\Delta T(2*CO_2)$ is defined as the temperature increase caused by a doubling of the atmospheric CO_2 equivalent concentration.

Scenario A (business as usual) portrays the continued trend of today with a doubling of CO_2 equivalent concentration in about the year 2025. Scenario B (low emissions) shows a reduced increase so that CO_2 equivalent doubles in about 2050, while Scenario C (control policies) represents an even smaller increase rate (CO_2 equivalent doubling in about 2080), with the concentration becoming constant after reaching the doubling value. The smallest increase with practically a stabilization of CO_2 equivalent concentration after 2030 occurs in Scenario D (accelerated policies); there a doubling of CO_2 equivalent is not reached until 2100[4].

[4] Note that the doubling times given by the IPCC (IPCC First Assessment Report - Overview 1990) are slightly different: for Scenario B it is 2040 and for Scenario C it is 2050.

2. EQUILIBRIUM RUNS

In these runs the oceanic heat storage is neglected which causes the time lags in the Earth's climate system. IMAGE makes use of Wigley & Schlesinger's (1985) relatively simple EBM consisting of two atmospheric boxes one over land with zero heat capacity, and the other over an oceanic mixed layer coupled to a diffusive deeper ocean. The basic equation of the model, describing the oceanic mixed layer temperature change, is given by

$$c_m * \frac{d\Delta T(t)}{dt} = \Delta Q(t) - \lambda * \Delta T(t) - \Delta F \qquad (1)$$

where:

c_m : effective heat capacity of the earth (in $Wym^{-2}\ °C^{-1}$)

ΔT : change in global surface temperature (in °C)

ΔQ : net change in the solar plus terrestrial radiation (in Wm^{-2}) at the top of the atmosphere (tropopause) due to the change of some external parameter[5], assuming present climate

ΔF : change in heat flux at the bottom of the mixed layer

λ : global climate sensitivity parameter or feedback parameter (in $Wm^{-2}\ °C^{-1}$)

t : time (in y)

ΔF is the change in heat flux at the bottom of the mixed layer. It can be dropped if Eq. (1) refers to the globe as one box. In equilibrium, the response of global temperature to external radiative forcing is assumed to be instantaneous; the left side of Eq. (1) is then zero, yielding

$$\Delta T(t) = \frac{\Delta Q(t)}{\lambda} \qquad (2)$$

To combine the global temperature changes with time given by IMAGE with those of a globally and annually averaged GCM which are usually plotted versus CO_2 equivalent concentrations, we need to adjust IMAGE so that it has the same climate sensitivity $\Delta T(2*CO_2)$ as the GCM. In the most simple case the adjustment of the IMAGE results can be accomplished in three steps:

---

[5] Parameters regarded as not controlled by the climate system (such as the solar luminosity and the anthropogenic influence on greenhouse gas concentrations in the atmosphere) are referred to as external parameters by Dickinson (1982). ΔQ is usually termed total radiative forcing.

a) calculation of the feedback parameter λ with the help of the climate sensitivity $\Delta T(2*CO_2)$ taken from the GCM in question

$$\lambda = \frac{\Delta Q(2*CO_2)}{\Delta T(2*CO_2)} \tag{3}$$

where:

$\Delta T(2*CO_2)$: climate sensitivity (in °C)

$\Delta Q(2*CO_2)$: radiative forcing for a doubled CO_2 equivalent concentration derived from Radiative Convective Models (RCMs); $\Delta Q = 4.32$ Wm^{-2} is used in IMAGE

b) calculation of the radiative forcing ΔQ according to Rotmans (1990)

$$\Delta Q(conc) = \frac{\Delta Q(2*CO_2)}{\ln 2} * \ln\left(\frac{conc}{conc_o}\right) \tag{4}$$

where:

conc(t) : CO_2 equivalent concentration (in ppm)

$conc_o$: CO_2 concentration (296ppm) in the year 1900, the assumed level for preindustrial times

c) calculation of ΔT = f(conc) with Eqs. (2), (3) and (4)

$$\Delta T(conc) = \frac{1}{\lambda} * \frac{\Delta Q(2*CO_2)}{ln2} * \ln\frac{conc}{conc_o} \tag{5}$$

or

$$\Delta T(conc) = \frac{\Delta T(2*CO_2)}{ln2} * \ln\frac{conc}{conc_o} \tag{6}$$

Figure 6 shows the equilibrium temperature response for $\Delta T(2*CO_2) = 2.5$°C as a function of atmospheric CO_2 equivalent concentration, according to Eq. (6).

In the case of an equilibrium run there is only one curve for all scenarios that relates temperature increase to CO_2 equivalent concentration. If the temperature changes calculated by IMAGE for the different scenarios were to be plotted versus CO_2 equivalent concentration (instead of time), they would all fall upon this curve. Note that the above adjustment with respect to λ can be also applied to smaller concentration intervals within the range of $1*CO_2$ to $2*CO_2$. By doing so, the equilibrium curve of IMAGE can be tuned stepwise in order to

optimally follow the corresponding GCM temperature curve.

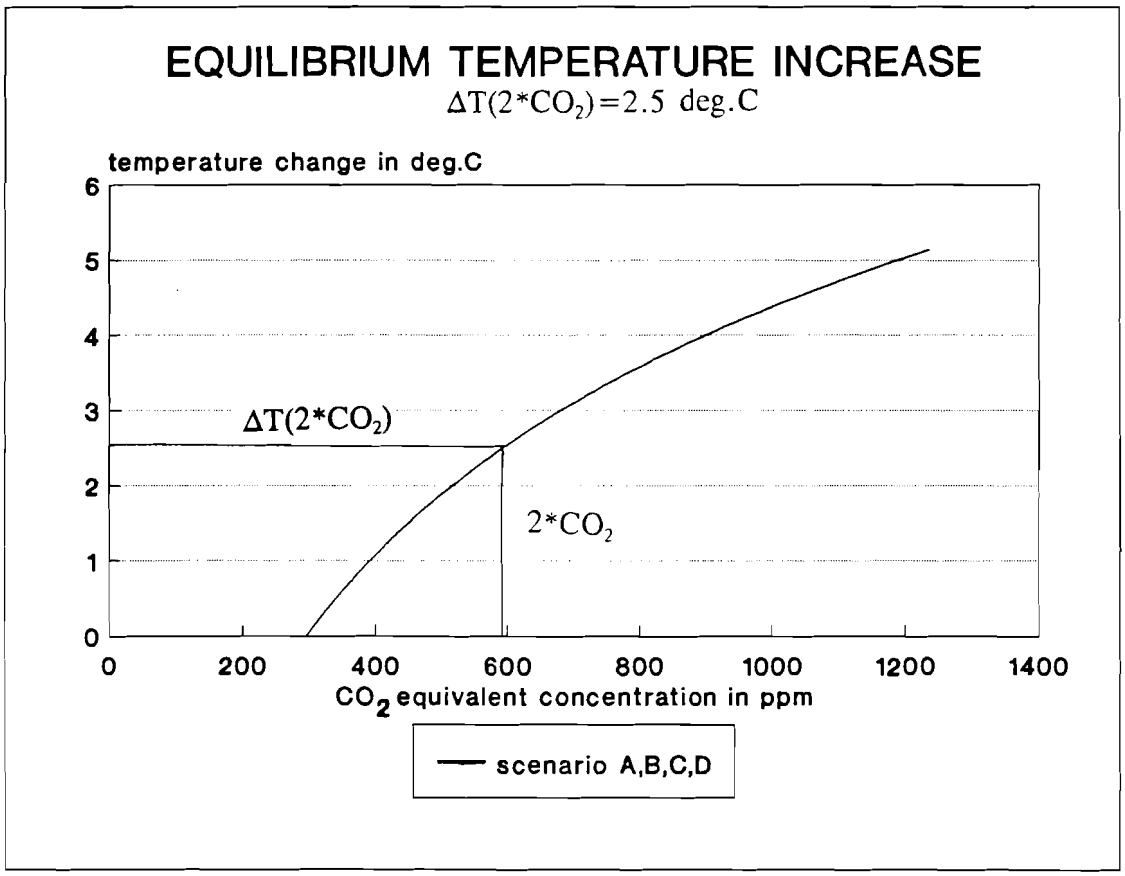

Figure 6: Equilibrium temperature change as a function of CO_2 equivalent concentration for a climate sensitivity $\Delta T(2*CO_2)=2.5°C$.

3. TIME-DEPENDENT RUNS

Time-dependent runs are used to simulate the effect of gradually changing CO_2 equivalent concentrations and are simulated in climate models by different scenarios of future greenhouse gas emissions or resulting atmospheric concentrations. In this chapter we will show how the global temperature response versus CO_2 equivalent concentration can be calculated analytically. Environmental impact modelers, for instance, might wish to make use of such a functional relationship.

3.1. Runs without a time lag caused by the deep ocean

The equilibrium simulations of GCMs are restricted to the atmosphere and oceanic mixed layer and thus ignore both the deep ocean and changes in oceanic circulation. Comparing these GCM runs with Energy Balance Model (EBM) runs which, in the equilibrium mode, incorporate neither the mixed layer nor the deep ocean gives an indication of the time lag caused by the mixed layer. The e-folding time is in the order of 5-10 years according to Schneider and Thompson (1981).

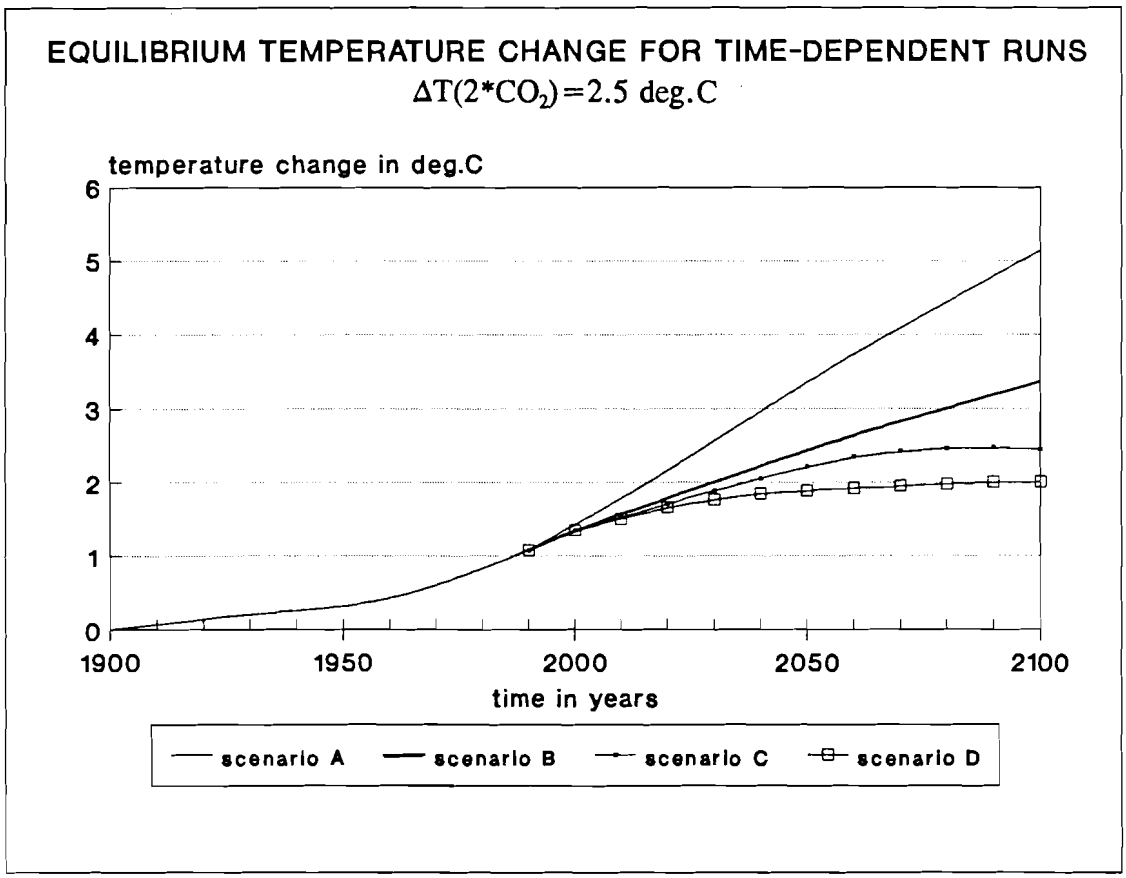

Figure 7: Time-dependent temperature change versus time for four scenarios and a climate sensitivity $\Delta T(2*CO_2)=2.5°C$, calculated by IMAGE disregarding the ocean.

Figure 7 shows the equilibrium temperature responses (without mixed layer and deep ocean) for the different scenarios as a function of time, as calculated by IMAGE. If they were plotted against CO_2 equivalent concentration, the temperature responses of all scenarios would fall upon the curve described by Eq. (6) (see also Figure 2).

3.2. Runs with a time lag caused by the deep ocean

The GCM runs include the heat storage by the deep ocean and all flux processes in the deep ocean. This results in a considerable time lag in the temperature response.

The temperature changes, as calculated by IMAGE for the four scenarios, taking into account the heat storage of the deep ocean, the flux processes between the deep ocean and the oceanic mixed layer as well as in the deep ocean itself by a 1-dimensional diffusive approach, are shown in Figure 8.

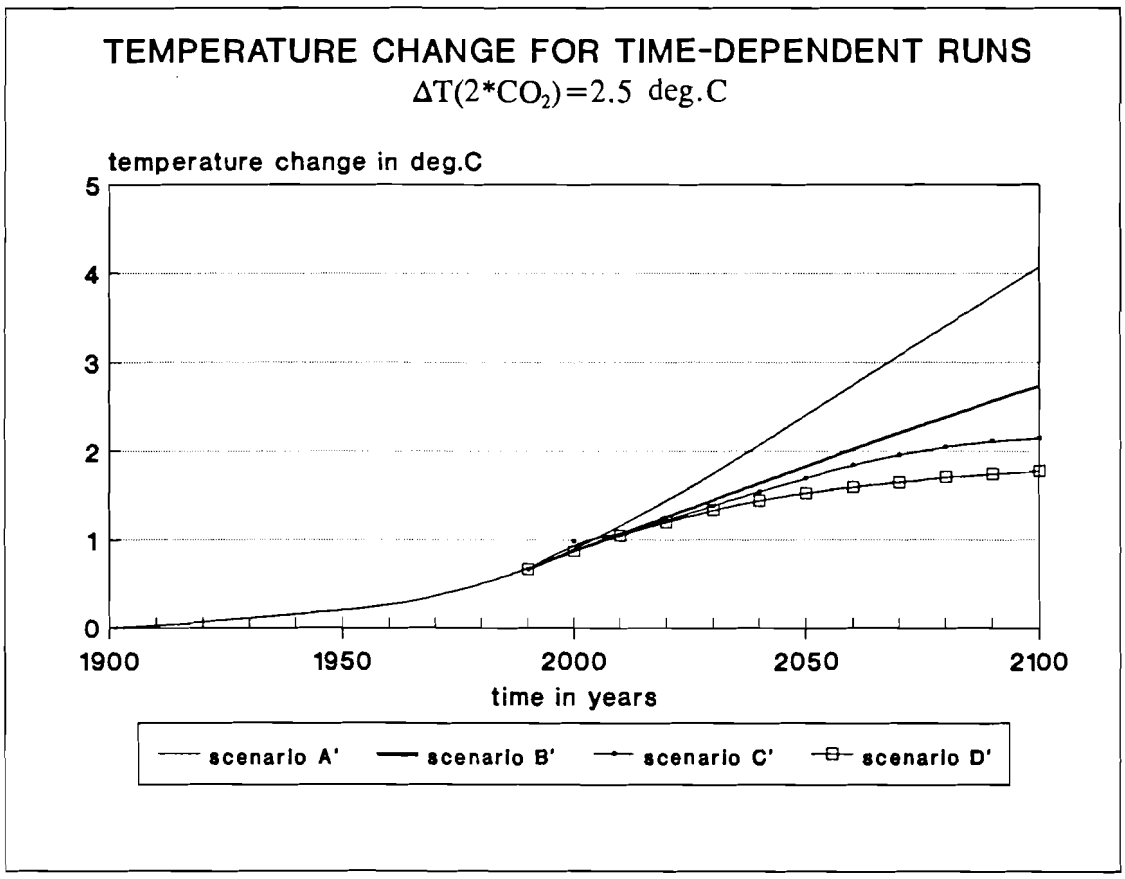

Figure 8: Time-dependent temperature change versus time for four scenarios and a climate sensitivity $\Delta T(2*CO_2)=2.5°C$, calculated by IMAGE taking into account the ocean.

ΔT_{td} : temperature change for the time-dependent run with deep ocean (in °C)

As stated above, we wish to provide a functional relationship $\Delta T_{td}=f(conc)$ for any concentration scenario. We assume that tuning IMAGE to any GCM by using the climate sensitivity and global feedback factor (see Chapter 2) will enable it to also simulate the respective GCM if run in a time-dependent mode (otherwise a further tuning procedure can be introduced). After using a simple fitting technique (an example will be given below) for both CO_2 equivalent concentration versus time and temperature change versus time, $conc=f_1(t)$ and $\Delta T_{td}=f_2(t)$, we then substitute the time t and as a result get $\Delta T_{td}=f(conc)$. For the four IMAGE scenarios the temperature changes versus CO_2 equivalent concentrations are presented in Figure 9.

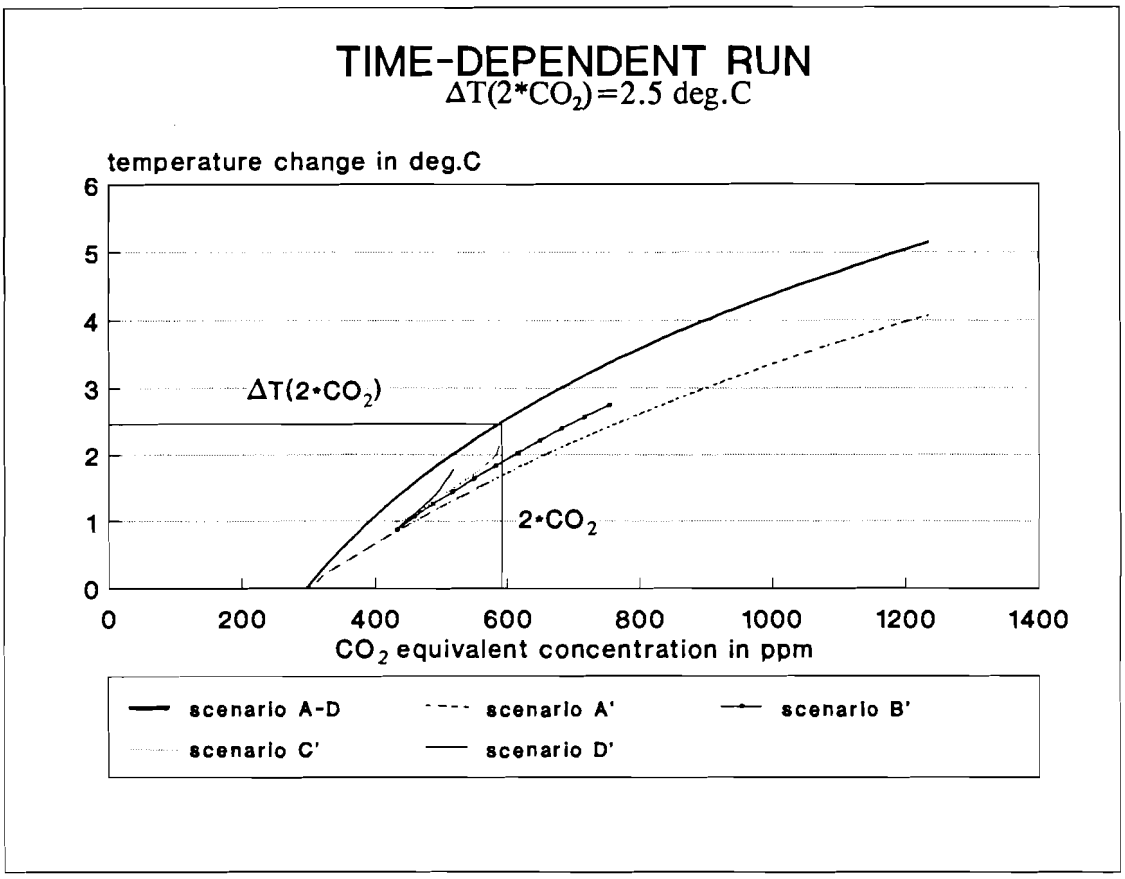

Figure 9: Temperature change versus CO_2 equivalent concentrations for a climate sensitivity $\Delta T(2*CO_2)=2.5°C$, as calculated by IMAGE.

In contrast to the runs without deep ocean there are differences among the scenarios with deep ocean: the smaller the rate of increase of the CO_2 equivalent concentration, the more time the system has to adapt to the disturbance and thus the closer the curve $\Delta T_{td}=$ f(conc) is to the equilibrium curve. This is shown by Figure 9, which is derived from the IMAGE runs. Note that the Scenarios A, B, C and D are equilibrium runs and A', B', C', D' are

time-dependent runs, which take the deep ocean and the resulting time lags into account. We now describe the methodology for four cases in which CO_2 equivalent concentrations vary with time.

a) Increasing CO_2 equivalent concentrations

Assume the function conc = $f_1(t)$ can be well described by an exponential function for scenarios such as A and B in which concentrations increase with time. We then can easily isolate the variable for time, t, from the equation below.

$$conc(t)=a*\exp[b(t-t_o)]+c \tag{7}$$

$$\frac{1}{b}\ln(\frac{conc(t)-c}{a})=t-t_o \tag{8}$$

where:

t_o : the year 1900

a, b, c : constants which depend upon the scenario (in ppm, y^{-1}, ppm)

If the time-dependent temperature increase is also assumed to be exponential, i.e.,

$$\Delta T_{td}(t)=k*\exp[l(t-t_o)]+m \tag{9}$$

where:

k, l, m : constants which depend upon the scenario (in °C, y^{-1}, °C),

we find after substituting Eq. (8) into Eq. (9):

$$\Delta T_{td}=m+k*(\frac{conc-c}{a})^{\frac{l}{b}} \tag{10}$$

Eq. (10) expresses ΔT_{td} as a function of concentration for exponentially increasing CO_2 equivalent concentration.

b) Stabilized CO_2 equivalent concentrations after increase

If the concentrations were to be stabilized at a certain level, the temperatures would continue to rise until the equilibrium temperatures for this concentration value were reached. One can visualize this process with help of Figures 10 and 11. Figure 10 shows how the temperature response for the transient run approaches the equilibrium response with time for an instantaneous doubling of CO_2 equivalent concentration. The vertical line from point 1 to 2 in Figure 11 shows the same process but for the temperature response being plotted versus CO_2 equivalent concentration.

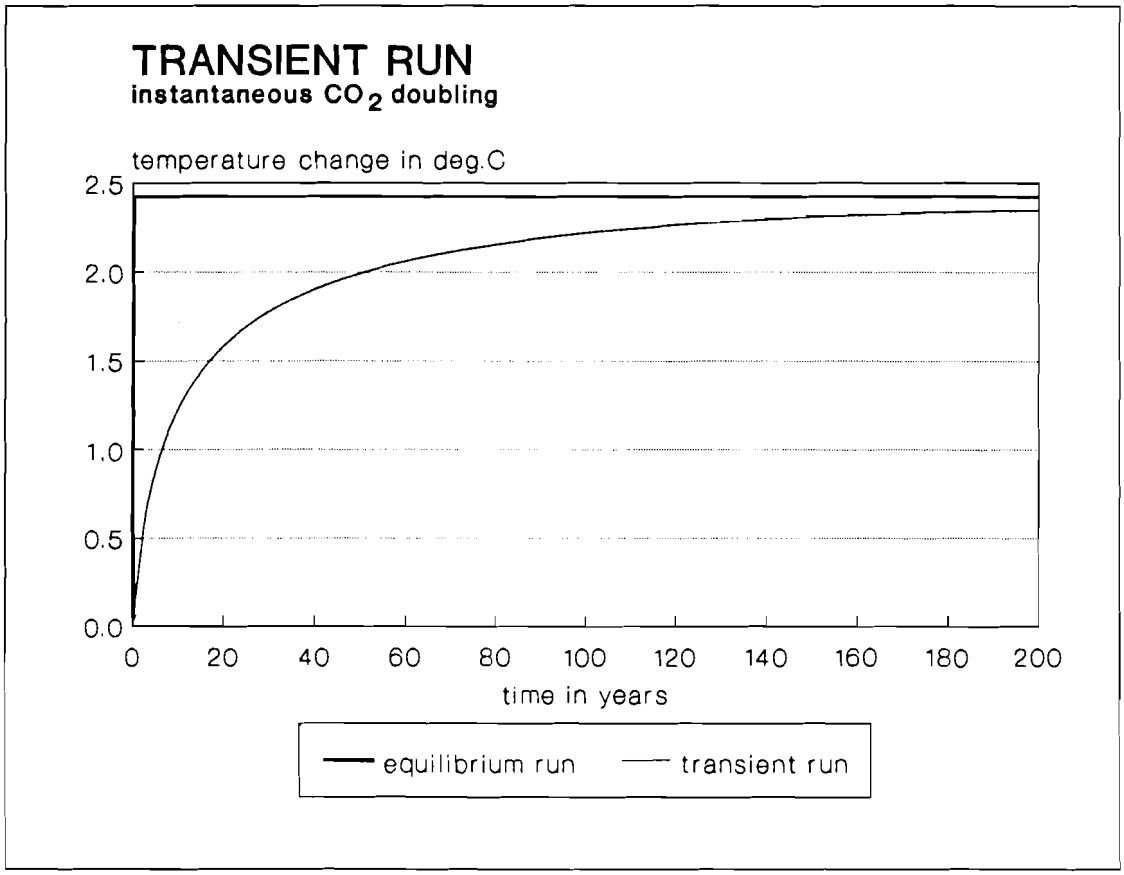

Figure 10: Temperature change for the transient run, calculated by IMAGE. Climate sensitivity $\Delta T(2*CO_2)=2.43°C$.

As shown in Figure 10, the equilibrium temperature is reached instantaneously if one neglects the oceanic mixed layer. In the transient run with deep ocean, 200 to 500 years are necessary to reach the equilibrium temperature (in Figure 10 the e-folding time is between 21 and 22 years according to Jonas et al., 1991), since the ocean delays the warming process considerably.

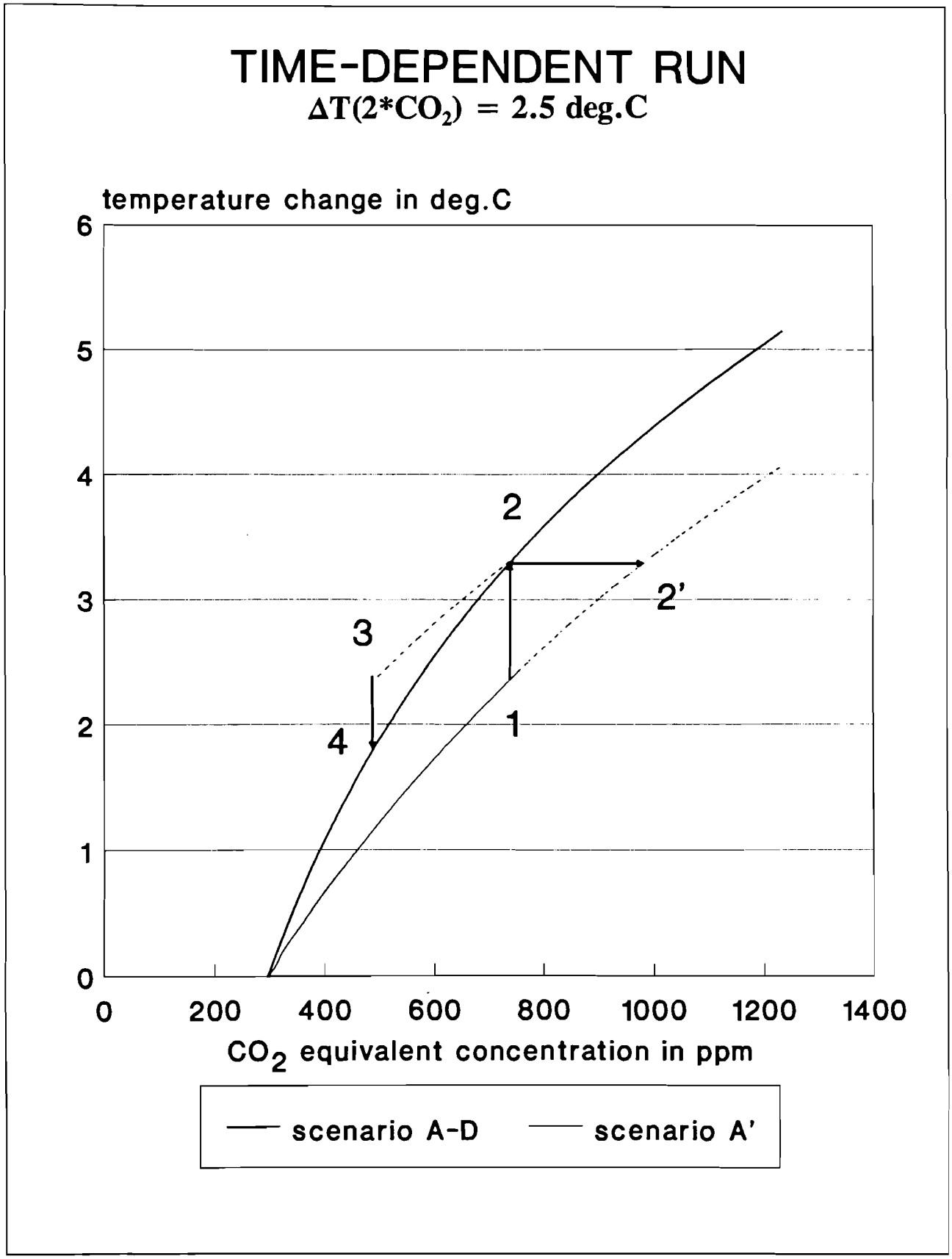

Figure 11: Schematic illustration: temperature change versus concentration.

The points in Figure 11 are

1 - temperature response which takes the ocean into account
2 - equilibrium temperature response
2'- temperature response which takes the ocean into account for a concentration corresponding to that of point 2
3 - point where the concentration is stabilized again
4 - equilibrium temperature response

Using Figures 10 and 11 we can find an expression to describe how quickly the temperature rises if the concentration were to be stabilized.

$$\Delta T_{td}(t) = \Delta T(conc) - [\Delta T(conc) - \Delta T_{td}(conc)] * \exp(gt) \qquad (11)$$

where:

$\Delta T_{td}(t)$: temperature change for a run with deep ocean, here as a function of time since the CO_2 equivalent concentration is constant (in °C)

$\Delta T_{td}(conc)$: temperature for the run with deep ocean at the time that the concentration becomes constant (in °C)

$\Delta T(conc)$: temperature for the run without deep ocean at the time that the concentration becomes constant (in °C)

g : constant, which can be found by fitting (in y^{-1})

All the quantities on the right hand side of Eq. (11) are derived with the help of IMAGE. The values for $\Delta T(conc)$ and $\Delta T_{td}(conc)$ come from Figure 11, the exponential term from Figure 10. If the concentration were to stabilize at another value, the corresponding temperature responses $\Delta T(conc)$ and $\Delta T_{td}(conc)$ would be replaced, the exponential term would not change.

c) Decreasing CO_2 equivalent concentrations

This is the most complex case because, at a given time, the transient temperature response may be above or below the equilibrium temperature response. It will depend upon whether or not the temperature had been at the equilibrium value at the time that the concentration had started to decrease. If it had reached the equilibrium temperature response, then the temperature response for the run with deep ocean will be above the equilibrium curve as shown in Figure 11 (see line going from point 2 to point 3). Now we apply Eq. (10) in a modified form:

$$\Delta T_{id}(conc) = m + k * \left(\frac{[conc + \Delta conc] - c}{a}\right)^{\frac{1}{b}} \qquad (12)$$

where:

Δconc : difference in concentration between points 2' and 2 (see Figure 11), (in ppm)

It is assumed that, where the deep ocean is taken into account, the temperature response follows the same shape of curve as when it was increasing. This defines the Δconc, which has to be added to the concentration at point 2 before the decreasing mode can be treated. Since, to our knowledge, the problem of temperature hysteresis has not been treated in the literature, we have to make this assumption. This may be questionable because the system might reveal what is called a "residual temperature response" (analogous to a residual magnetization) after the CO_2 equivalent concentration has returned to its initial value.

d) Stabilized concentrations after a decrease

In this case, the temperature changes as described in case b). It decreases if the temperature for the run is already greater than the equilibrium temperature, or it rises to the equilibrium temperature value if it is still less. In Figure 11, only the first case is shown (see line going from point 3 to point 4).

To treat a case in which there are several successive changes (e.g., increase, stabilization, decrease) in the atmospheric CO_2 equivalent concentration, the problem should be divided into intervals accordingly, each being described by a separate equation.

4. CONSIDERATION OF DIFFERENT CLIMATE SENSITIVITIES

According to the IPCC, the climate sensitivity of GCMs usually lies between 1.5 and 4.5 °C. However, we also wish to consider a climate sensitivity of 0.5 °C, as suggested recently by Lindzen (1990) and Schlesinger (1991).

4.1. Runs without time lag caused by the deep ocean

To change the climate sensitivity $\Delta T(2*CO_2)$ for the run without ocean, one can make direct use of Eq. (6).

4.2. Runs with time lag caused by the deep ocean

IMAGE provides the corresponding functions $\Delta T_{td}=f(t)$ for different climate sensitivities $\Delta T(2*CO_2)$ = 0.5, 1.5, 2.5, 3.5, 4.5°C. In Figure 12, they are shown for Scenario A'.

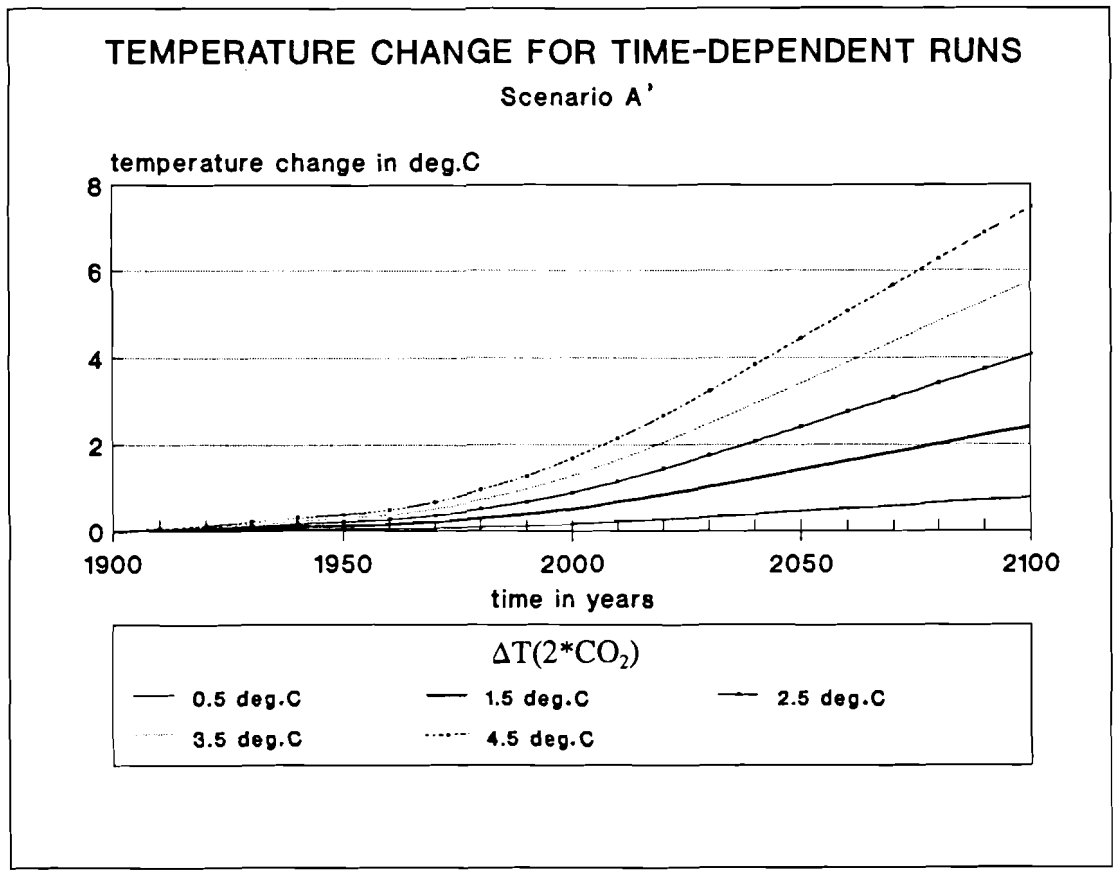

Figure 12: Temperature change for a time-dependent run calculated by IMAGE (Scenario A') for the climate sensitivities $\Delta T(2*CO_2)$= 0.5, 1.5, 2.5, 3.5, 4.5°C.

If the climate sensitivity of the GCM lies between two of the sensitivities mentioned above, it is necessary to use a simple interpolation technique as depicted in Figure 13. With the help of the climate sensitivity of the GCM, $\Delta T_{new}(2*CO_2)$, its time-dependent temperature

response ΔT_x can be calculated as a function of time according to

$$\frac{\Delta T_a(t)-\Delta T_b(t)}{\Delta T_a(2*CO_2)-\Delta T_b(2*CO_2)}=\frac{\Delta T_a(t)-\Delta T_x(t)}{\Delta T_a(2*CO_2)-\Delta T_{new}(2*CO_2)} \quad (13)$$

$$\Delta T_x(t)=\Delta T_a(t)-(\Delta T_a(2*CO_2)-\Delta T_{new}(2*CO_2))*\frac{\Delta T_a(t)-\Delta T_b(t)}{\Delta T_a(2*CO_2)-\Delta T_b(2*CO_2)} \quad (14)$$

where:

ΔT_a : time-dependent temperature response resulting from the climate sensitivity $\Delta T_a(2*CO_2)$, (in °C)

ΔT_b : time-dependent temperature response resulting from the climate sensitivity $\Delta T_b(2*CO_2)$, (in °C)

ΔT_x : unknown temperature response for the climate sensitivity $\Delta T_{new}(2*CO_2)$, (in °C)

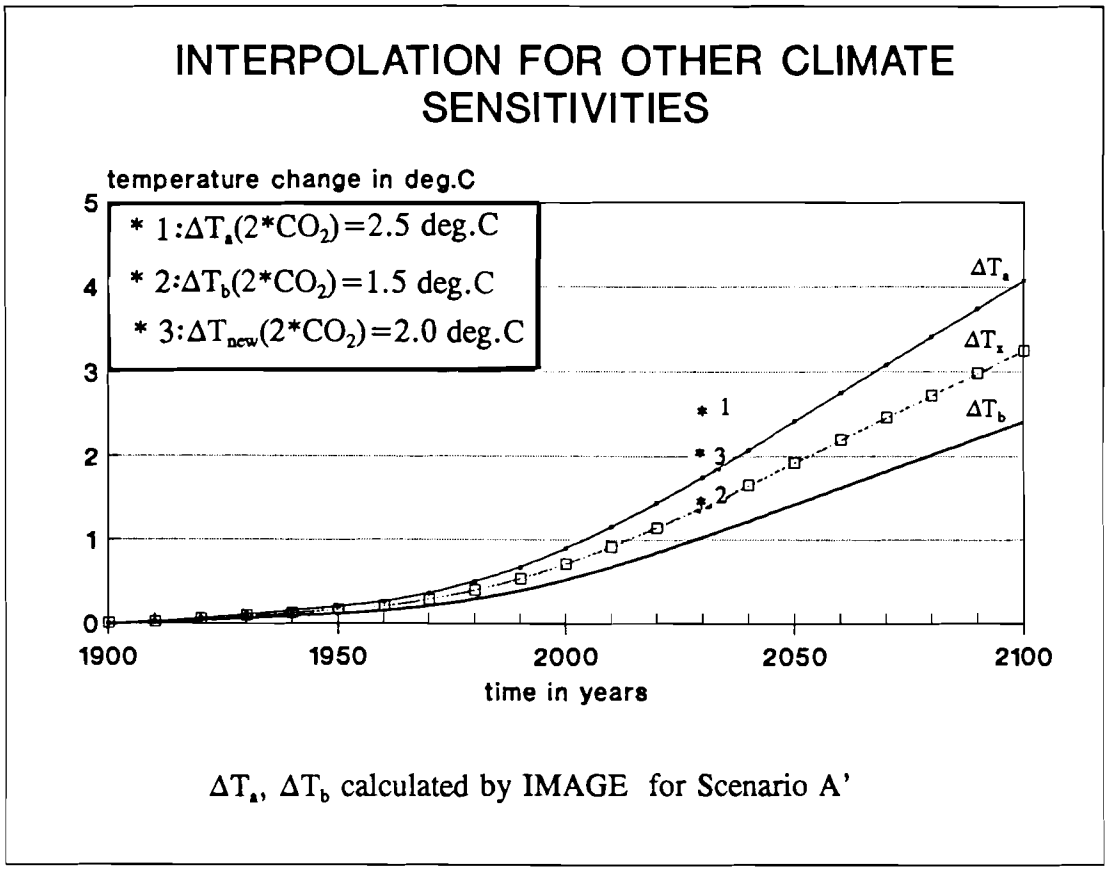

Figure 13: Linear interpolation of the time-dependent GCM temperature response ΔT_x for a climate sensitivity $\Delta T_{new}(2*CO_2)$, which is between $\Delta T_a(2*CO_2)=1.5$°C and $\Delta T_b(2*CO_2)=2.5$°C of IMAGE, e. g. $\Delta T_{new}(2*CO_2)=2.0$°C.

5. REGIONALIZATION

Both the geographical and the seasonal distribution of temperature change are very important for estimating the economic and the social impacts of climate change. However, in this chapter we consider only the geographical distribution. Our aim is to outline a methodology which is potentially suited for linking IMAGE to the regional temperature scenarios produced by a GCM.

The global climatic patterns are related to the variation in the amount of solar energy reaching the Earth's surface. The important factors which influence regional climate are

- the location of the region relative to ocean and continental influences

- the atmospheric circulation, including the semi-permanent wind and pressure belts

- oceanic currents

- the elevation above sea level

- orographic barriers.

5.1. Runs without a time lag caused by the deep ocean

In these runs the regional patterns of temperature change in different GCMs are similar with respect to time. Despite the different parameterizations in the GCMs, there are common features in the output maps from all models (IPCC 1990).

The regional mean ΔT values for different areas are needed from the GCM outputs. We assume that initially (i.e., at $1*CO_2$ equivalent concentration) the global and regional temperature changes are zero. Of course, at this time there is a geographical variation of temperature, but there is still no temperature change due to an enhanced CO_2 equivalent concentration. For a doubled CO_2 equivalent concentration, the GCMs provide regional climate sensitivities, the temperature changes for a doubled CO_2 equivalent concentration for particular regions. We assume that the relative magnitude of temperature changes in different regions due to any anthropogenic forcing between $1*CO_2$ and $2*CO_2$ equivalent concentrations follows the regional patterns of temperature sensitivities in both equilibrium and time-dependent runs. The following conditions should then hold

$$\Delta T_G(2*CO_2)=\sum_{i=1}^{n} w_i*\Delta T_R(2*CO_2) \qquad (15)$$

and

$$\Delta T_G(conc) = \sum_{i=1}^{n} w_i * \Delta T_R(conc) \qquad (16)$$

where:

$\Delta T_G(2*CO_2)$: global climate sensitivity (in °C)

$\Delta T_R(2*CO_2)$: climate sensitivity of the GCM for a particular region (in °C), (from the GCM output)

w_i : appropriate weighting (e.g. area weighting)

$\Delta T_G(conc)$: global temperature change for an arbitrary CO_2 equivalent concentration, (in °C)

$\Delta T_R(conc)$: regional temperature change for an arbitrary CO_2 equivalent concentration, (in °C)

As a first approach we propose a relationship similar to Eq. (6) but on a regional level

$$\Delta T_R(conc) = \Delta T_R(2*CO_2) * \frac{\ln(\frac{conc}{conc_o})}{\ln 2} \qquad (17)$$

Here we assume that the global logarithmic character of $\Delta T_G(conc)$ with respect to CO_2 equivalent concentration also applies for $\Delta T_R(conc)$. In fact, $\Delta T_R(2*CO_2)$ can be considered as a potential tuning parameter that allows the IMAGE equilibrium curve to follow that of the GCM. (It can be readjusted for different CO_2 equivalent concentration intervals as it could be done with $\Delta T_G(2*CO_2)$ through the global feedback parameter λ). In future research we propose to study this or a similar functional relationship that satisfies the boundary condition given in Eqs. (15) or (16).

5.2. Runs with a time lag caused by the deep ocean

The distribution of the regional values in a GCM run which includes the deep ocean is somewhat more difficult. There are many differences among the results of the various GCMs. However, the IPCC Report states that:

- the regional patterns of time-dependent runs resemble those of an equilibrium simulation for an atmospheric model, but with a reduced magnitude (IPCC, 1990, p. 177).

- apart from areas where the oceanic thermal inertia is large (as in the North Atlantic) the solution from the run without deep ocean can be scaled and used as approximations to the time-dependent response (IPCC, 1990, p. 137).

These findings are supported by the Report of the First Session of the WCRP Steering Group on Climate Modelling (1991) where it is stated that:

- in the GFDL coupled ocean-atmosphere model (Stouffer, 1989), the distribution of the change in surface air temperature at the time of CO_2 equivalent doubling resembles the equilibrium response to $2*CO_2$ of an atmospheric mixed layer ocean model, with the exception of the northern North Atlantic and the circum-polar flow in the southern hemisphere (WCRP-55, 1991, p.4).

Hence, we propose that the regionalization for the run with ocean could be carried out in two steps:

1) We could consider these GCMs for which the regional distribution of the run with ocean is similar to the run without deep ocean, say with the help of a Geographical Information System (GIS). One could then use the same regionalization procedure as for the run without deep ocean. One must take the reduced magnitude into account, which can be expressed through:

$$\frac{\Delta T_{G(td)}(conc)}{\Delta T_{R(td)}(conc)} = \frac{\Delta T_G(conc)}{\Delta T_R(conc)} \tag{18}$$

Rearranging to solve for $\Delta T_{R(td)}(conc)$ for any concentration gives:

$$\Delta T_{R(td)}(conc) = \frac{\Delta T_{G(td)}(conc) * \Delta T_R(conc)}{\Delta T_G(conc)} \tag{19}$$

where:

$\Delta T_{G(td)}(conc)$: global temperature change for the run with ocean (in °C)

$\Delta T_{R(td)}(conc)$: regional temperature change for the run with ocean (in °C)

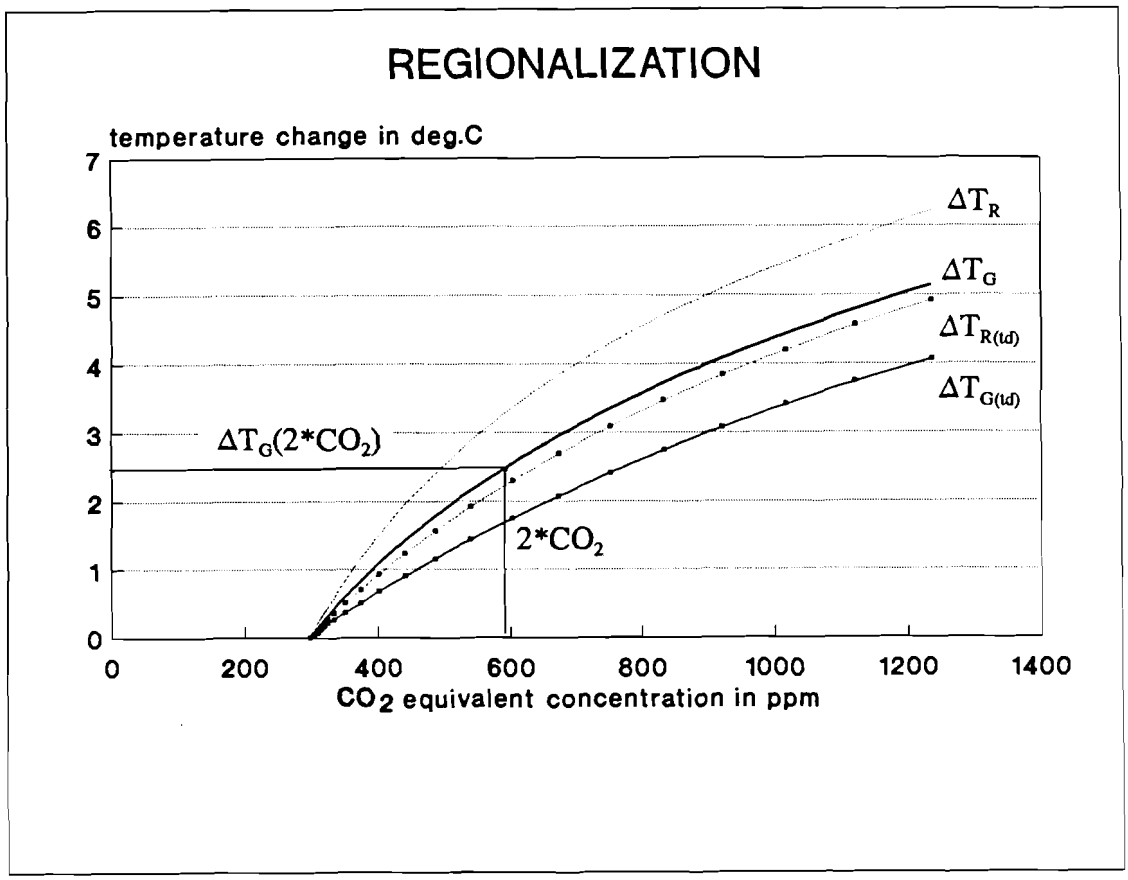

Figure 14: Regionalization using temperature ratios.

2) The above approximations implicitly account for regional fractions of land and ocean which are close to the global fraction of land and ocean (29% land, 71% ocean). However, there might be a need to correct for the higher temperature responses over continents (MPI Report, 1991). This could be achieved by further correcting Eq. (19) for fractions of land and ocean of the regions in question.

6. SUMMARY AND OUTLOOK

It was the objective of this paper to outline a methodology for combining the surface temperature outputs of three-dimensional GCMs with those of the zero-dimensional but time-dependent IMAGE model. We approached the problem in two steps. In the first we proposed tuning the IMAGE results to a globally and annually averaged GCM, i. e., to make the equilibrium and the time-dependent temperature responses of IMAGE follow the corresponding curves of the GCM. In the most simple case, this is achieved by adjusting the global feedback factor. Figure 15 indicates the potential of IMAGE of calculating the first order temperature response of a globally averaged GCM. (Note that only the climate sensitivity of the GCM was taken over; no further tuning was involved. Unfortunately, only the time-dependent run of the GCM and the climate sensibility were available, but not the complete equilibrium run.) In the second step we extended the methodology developed on the global scale to regions. This step is more subject than the first step to scientific uncertainty with respect to both methodology and range of temperature change. We proposed a simple functional relationship, similar to the global one, which enables IMAGE to calculate an equilibrium temperature response for a given region with the help of the respective regional climate sensitivity of the GCM and to follow its equilibrium temperature curve.

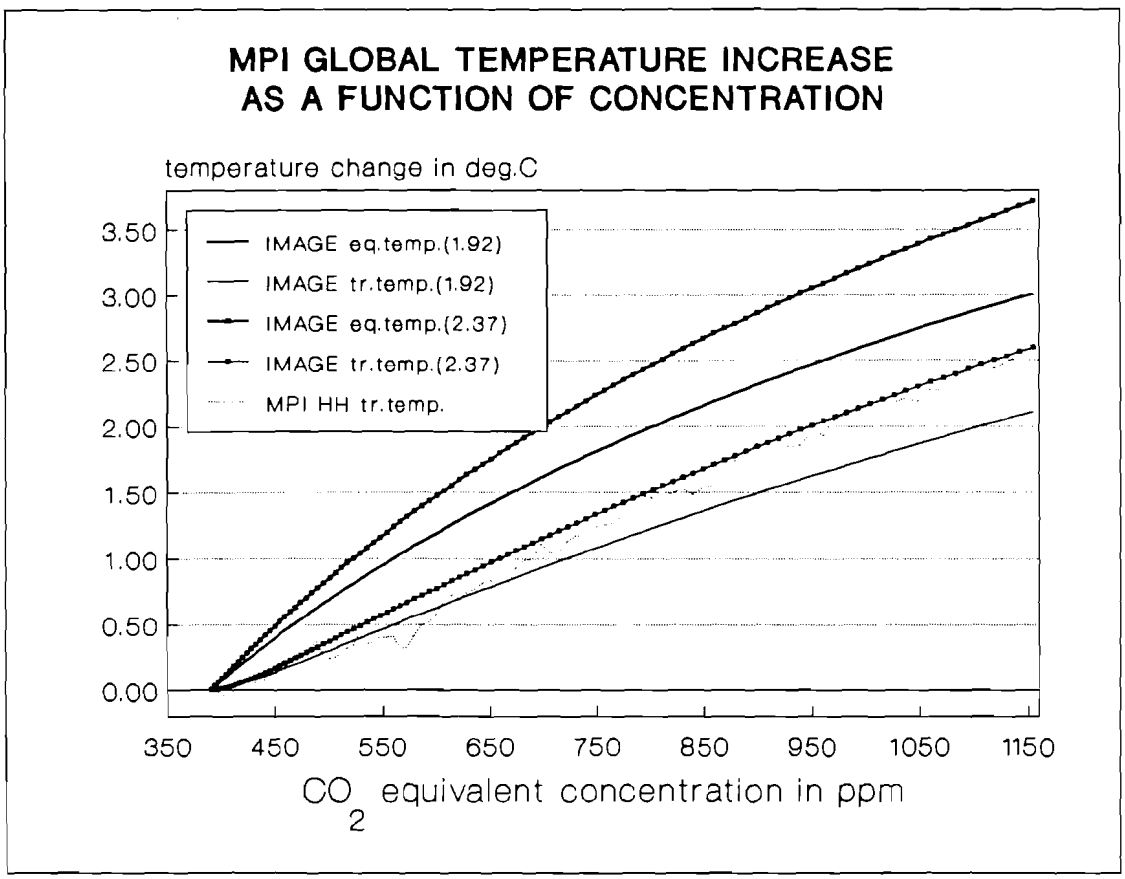

Figure 15: Comparison between IMAGE and the GCM of the Max-Planck-Institute (MPI) in Hamburg (Cubasch et al., 1991). The GCM is forced according to their Scenario A which resembles Scenario A of IMAGE. (Unfortunately, the MPI model offers several options on how to define the climate sensitivity. This is because of their 100y control run which shows a negative temperature drift. However, if the complete equilibrium run is known, such a problem can be avoided.)

The regional time-dependent temperature response of IMAGE is then derived with the help of a simple ratio method where we take advantage of the fact that the regional patterns of a time-dependent temperature change generally resemble those of an equilibrium simulation for an atmospheric model, though uniformly reduced in magnitude due to the time lag caused by the deep ocean. It is expected that the regional time-dependent temperature curve of IMAGE will simulate well enough the corresponding curve of the GCM.

In any case, the proposed tuning procedure will be further investigated and tested with different GCMs. If successful, this adaptation of the IMAGE model will be able to give quick first order estimates on global and regional surface temperature changes for global emission or concentration scenarios other than that used in the tuning process. It could then be a valuable tool for national and international decisionmakers and research groups dealing with the impacts from climate change without resorting to costly GCM runs.

REFERENCES

Akin, W.E. 1991. *Global Patterns: Climate, Vegetation and Soils*. University of Oklahoma Press, U.S.

Antonovsky, M.Y., Bukhshtaber, V.M. and A.A. Zubenko. 1988. *Statistical Analysis of Long-Term Trends in Atmospheric Carbone Dioxide Concentrations at Baseline Stations*. Working Paper WP-122. International Institute for Applied Systems Analysis, Laxenburg, Austria.

Baule, B. 1963. *Die Mathematik des Naturforschers und Ingenieurs*. Bd.II, S. Hirzel Verlag Leipzig, Germany.

Cubasch et al. 1991. Simulation of the greenhouse effect with coupled ocean-atmosphere models. *Cray Channels*, Winter 1991:6-9.

Dickinson, R.E. 1982. Modeling climate changes due to carbon dioxide increases. Pages 101-133 in W.C. Clark (ed.), *Carbon Dioxide Review*. Oxford University Press, New York.

Harrison, S.P. 1990. *An Introduction to General Circulation Modelling Experiments with Raised CO_2*. Working Paper WP-27, International Institut for Applied Systems Analysis, Laxenburg, Austria.

Hendersen-Sellers, A. and K.McGuffie. 1987. *A Climate Modelling Primer*. John Wiley and Sons, Chichester, U.K.

Intergovernmental Panel on Climate Change IPCC. 1990. *Climate Change - The IPCC Scientific Assessment*. Report prepared for the IPCC by Working Group 1. J.T.Houghton, G.J. Jenkins and J.J. Ephraums (eds.), Cambridge University Press, Cambridge, U.K.

Intergovernmental Panel on Climate Change IPCC. August 1990. *IPCC First Assessment Report - Volume I*. Report.

Intergovernmental Panel on Climate Change IPCC. 1990. *Emission Scenarios*. Report on the Expert Group on Emission Scenarios (RSWG Steering Committee, Task A).

Intergovernmental Panel on Climatic Change. 1990. IPCC First Assessment Report - Overview, Report.

Jonas, M., den Elzen, M.G.J. and K. Olendrzyński, 1991. *A time-dependent zonally averaged Energy Balance Model to be incorporated into IMAGE (Integrated Model to Assess of the Greenhouse Effect (IMAGE)*. Collaborative Paper CP-16. International Institute for Applied Systems Analysis, Laxenburg, Austria.

Leemans, R. 1990. *Possible Changes in Natural Vegetation Patterns due to Global Warming*. Working Paper WP-108. International Institute for Applied Systems Analysis, Laxenburg, Austria.

Lindzen, R.S. 1990. Some coolness concerning global warming. *Bulletin American Meteorological Society* 71, No.3:288-299.

Manabe, E. and R.J. Stouffer. 1988. Two Stable Equilibria of a Coupled Ocean-Atmosphere Model. *Journal of Climate* 1:841-866.

Mikolajewicz, U., Santer, B.D. and E. Maier-Reimer. 1990. Ocean response to greenhouse warming. *Nature* 345:589-593.

MPI-REPORT. 1991. *Time-dependent Greenhouse Warming Computations with a Coupled Ocean-Atmosphere Model.* Report No.67. Max-Planck-Institute für Meteorologie Hamburg, Germany.

Rotmans, J. 1990. *IMAGE - An Integrated Model to Assess the Greenhouse Effect*, Kluwer Academic Publishers, Dordrecht, The Netherlands.

Rotmans, J., de Boois, H. and R.J. Swart. 1990. An Integrated Model for the Assessment of the Greenhouse Effect: The Dutch Approach. *Climate Change* 16:331-356.

Rotmans, J., Swart R.J. and M.G.J. den Elzen. 1991. *Stabilizing Atmospheric Concentrations: Towards International Methane Control.* Report nr. 222901008. National Institute for Public Health and Environmental Protection (RIVM), Bilthoven, The Netherlands.

Sausen, R., Barthel, K. and K. Hasselmann. 1988. Coupled ocean-atmosphere models with flux correction. *Climate Dynamics* 2:145-163.

Schlesinger, M.E. and X. Jiang. 1991. Revised projection of future greenhouse warming. *Nature* 350:219-221.

Schneider, S.H. and S.L.Thompson. 1981. Atmospheric CO_2 and climate: importance of the transient response. *Journal of Geophysical Research* 86(C4):3135-3147.

Washington, W.M. and G.A.Meehl. 1989. Climate sensitivity due to increased CO_2: experiments with a coupled atmosphere and ocean general circulation model. *Climate Dynamics* 4:1-38.

WCRP Steering Group on Global Climate Modelling, 1991. *Report of first session of the WCRP Steering Group on Global Climate Modelling.* Report WCRP-55. World Climate Programme Research, Geneva, Switzerland, 5.- 8. November 1990.

Wigley, T.M.L. and M.E. Schlesinger. 1985. Analytical solution for the effect of increasing CO_2 on global mean temperature. *Nature* 315:649-652.